Neurobiology of Aging xxx (2019) 1–9

Contents lists available at ScienceDirect

Neurobiology of Aging

journal homepage: www.elsevier.com/locate/neuaging

Dysregulated Fc gamma receptor–mediated phagocytosis pathway in Alzheimer's disease: network-based gene expression analysis

Young Ho Park[a,b], Angela Hodges[c], Shannon L. Risacher[a], Kuang Lin[c], Jae-Won Jang[d], Soyeon Ahn[e], SangYun Kim[b], Simon Lovestone[f], Andrew Simmons[c], Michael W. Weiner[g,h], Andrew J. Saykin[a,i,**,1], Kwangsik Nho[a,j,*,1], for the AddNeuroMed consortium and the Alzheimer's Disease Neuroimaging Initiative[2]

[a] Department of Radiology and Imaging Sciences, and the Indiana Alzheimer Disease Center, Indiana University School of Medicine, Indianapolis, IN, USA
[b] Department of Neurology, Seoul National University Bundang Hospital and Seoul National University College of Medicine, Seongnam, Republic of Korea
[c] Institute of Psychiatry, Psychology & Neuroscience, King's College London, London, UK
[d] Department of Neurology, Kangwon National University Hospital, Chuncheon, Republic of Korea
[e] Medical Research Collaborating Center, Seoul National University Bundang Hospital, Seongnam, Republic of Korea
[f] Department of Psychiatry, University of Oxford, Oxford, UK
[g] Departments of Radiology, Medicine, and Psychiatry, University of California-San Francisco, San Francisco, CA, USA
[h] Department of Veterans Affairs Medical Center, San Francisco, CA, USA
[i] Department of Medical and Molecular Genetics, Indiana University School of Medicine, Indianapolis, IN, USA
[j] Center for Computational Biology and Bioinformatics, Indiana University School of Medicine, Indianapolis, IN, USA

ARTICLE INFO

Article history:
Received 26 August 2019
Received in revised form 15 November 2019
Accepted 3 December 2019

Keywords:
Alzheimer's disease
Transcriptome
PRKCD
Network
Coexpression
Phagocytosis

ABSTRACT

Transcriptomics has become an important tool for identification of biological pathways dysregulated in Alzheimer's disease (AD). We performed a network-based gene expression analysis of blood-based microarray gene expression profiles using 2 independent cohorts, Alzheimer's Disease Neuroimaging Initiative (ADNI; N = 661) and AddNeuroMed (N = 674). Weighted gene coexpression network analysis identified 17 modules from ADNI and 13 from AddNeuroMed. Four of the modules derived in ADNI were significantly related to AD; 5 modules in AddNeuroMed were significant. Gene-set enrichment analysis of the AD-related modules identified and replicated 3 biological pathways including the Fc gamma receptor–mediated phagocytosis pathway. Module-based association analysis showed the AD-related module, which has the 3 pathways, to be associated with cognitive function and neuroimaging biomarkers. Gene-based association analysis identified *PRKCD* in the Fc gamma receptor–mediated phagocytosis pathway as being significantly associated with cognitive function and cerebrospinal fluid biomarkers. The identification of the Fc gamma receptor–mediated phagocytosis pathway implicates the peripheral innate immune system in the pathophysiology of AD. *PRKCD* is known to be related to neurodegeneration induced by amyloid-β.

1. Introduction

Alzheimer's disease (AD) is the most common form of dementia (Alzheimer's Association, 2018). Although AD is classically viewed primarily as a neurodegenerative central nervous system disease, many systemic manifestations suggest that AD is a multifactorial disease that affects both the brain and periphery (Morris et al., 2014). The systemic manifestations generally parallel the progressive functional decline associated with neurodegeneration (Morris et al., 2014). However, some systemic manifestations are also observable before the presence of clinical symptoms in AD (Vidoni et al., 2011).

Because blood interacts with every organ in the body, including the brain, blood-based profiles may provide an accessible and

* Corresponding author at: Department of Radiology and Imaging Sciences, Center for Neuroimaging, Indiana University School of Medicine, Indianapolis, IN, USA. Tel.: +1-317-963-7503; fax: +1-317-963-7547.
** Corresponding author at: Department of Radiology and Imaging Sciences, Center for Neuroimaging, Indiana University School of Medicine, Indianapolis, IN, USA. Tel.: +1-317-278-6947; fax: +1-317-274-1067.
E-mail addresses: asaykin@iu.edu (A.J. Saykin), knho@iu.edu (K. Nho).
[1] These authors contributed equally to the manuscript.
[2] Data used in preparation of this article were obtained from the Alzheimer's Disease Neuroimaging Initiative (ADNI) database (adni.loni.usc.edu). As such, the investigators within the ADNI contributed to the design and implementation of ADNI and/or provided data but did not participate in analysis or writing of this report. A complete listing of ADNI investigators can be found at: http://adni.loni.usc.edu/wp-content/uploads/how_to_apply/ADNI_Acknowledgement_List.pdf.

0197-4580/$ – see front matter © 2019 Elsevier Inc. All rights reserved.
https://doi.org/10.1016/j.neurobiolaging.2019.12.001

effective tool for assessing the complex interplay between the brain and the periphery in the pathogenesis of AD (Mohr and Liew, 2007). Among blood-based biomarkers, the transcriptome uniquely reflects both fixed genetic effects and dynamic environmental effects (Gladkevich et al., 2004; Tylee et al., 2013). There have been several studies investigating blood transcriptomic profiles in AD, which reported biological pathways including stress and immune responses (Bai et al., 2014; Booij et al., 2011; Chen et al., 2011; Fehlbaum-Beurdeley et al., 2012; Han et al., 2013; Kálmán et al., 2005; Lunnon et al., 2013, 2012; Maes et al., 2007; Naughton et al., 2015; Roed et al., 2013; Rye et al., 2011). However, many of the studies analyzed only a small number of samples, and their findings were not replicated in independent cohorts. Furthermore, most of the aforementioned studies evaluated differential expressions only at the level of individual genes. Because genes with similar function tend to have correlated expression (Eisen et al., 1998), network-based approaches can better elucidate the molecular mechanisms underlying complex brain disorders (Dragomir et al., 2018).

In this study, using 2 independent cohorts, we performed blood-based gene coexpression network analysis to identify AD-related modules. We then performed pathway-based enrichment analysis to determine biological functions characteristic of these AD-related modules and association analysis of the AD-related modules and genes belonging to the biological pathways with fluid and neuroimaging biomarkers for AD. For fluid biomarkers for AD, we used the concentration of amyloid-β_{42} ($A\beta_{42}$), phosphorylated tau_{181p} (p-tau), and total tau (t-tau) in cerebrospinal fluid (CSF) (Kang et al., 2015). For neuroimaging biomarkers for AD, we used a global cortical measure of amyloid burden measured from [^{18}F] florbetapir PET scans (Ramanan et al., 2014) and hippocampal volume measured from MRI scans (Potkin et al., 2009). Genetic data were also used for gene-based association analysis and expression quantitative trait locus (eQTL) analysis (Rockman and Kruglyak, 2006).

2. Material and methods

2.1. Participants

Data used in the study were obtained from the Alzheimer's Disease Neuroimaging Initiative (ADNI) and AddNeuroMed cohorts as discovery and replication samples, respectively. The ADNI was launched in 2003 as a public-private partnership, led by principal investigator Michael W. Weiner, MD. The primary goal of ADNI has been to test whether serial MRI, PET, other biological markers, and clinical and neuropsychological assessment can be combined to accurately capture the progression of mild cognitive impairment (MCI) and early AD. The AddNeuroMed is a cross-European, public/private consortium developed for AD biomarker discovery (Lovestone et al., 2009). The diagnosis of AD was made clinically using National Institute of Neurological and Communicative Disorders and Stroke and the Alzheimer's Disease and Related Disorders Association criteria for probable AD (McKhann et al., 1984). The diagnosis of MCI was made according to the presence of objective memory impairment but without meeting the criteria for dementia. Written informed consent was obtained at the time of enrollment and included permission for analysis and data sharing. The protocol and informed consent forms were approved by each participating sites' institutional review board.

2.2. Genotyping and imputation

Genotyping for ADNI and AddNeuroMed was performed using blood genomic DNA samples and Illumina GWAS array platforms (Illumina Human610-Quad BeadChip, Illumina HumanOmniExpress BeadChip, and Illumina HumanOmni 2.5M BeadChip) (Furney et al., 2011; Saykin et al., 2015). *APOE* genotyping was separately conducted using standard methods as described previously to yield the *APOE* $\varepsilon4$ allele defining single-nucleotide polymorphisms (SNPs) (rs429358, rs7412) (Furney et al., 2011; Saykin et al., 2015). Using PLINK 1.9 (www.cog-genomics.org/plink2/) (Purcell et al., 2007), we performed standard quality control (QC) procedures for samples and SNPs as described previously (Lee et al., 2018): (1) for SNP, SNP call rate $<$ 95%, Hardy-Weinberg p-value $< 1\times10^{-6}$, and minor allele frequency $<$ 1%; (2) for sample, sex inconsistencies and sample call rate $<$ 95%. Furthermore, to prevent spurious association due to population stratification, we selected only non-Hispanic participants of European ancestry, which clustered with HapMap CEU (Utah residents with Northern and Western European ancestry from the CEPH collection) or Toscani in Italia populations using multidimensional scaling analysis (Price et al., 2006; Thorisson et al., 2005). After QC procedures, as ADNI and AddNeuroMed used different genotyping platforms, we imputed ungenotyped SNPs separately in each platform using Markov Chain Haplotyping with the Haplotype Reference Consortium data as a reference panel (Li et al., 2010; McCarthy et al., 2016). After the imputation, we imposed an r^2 value equal to 0.30 as the threshold to accept the imputed genotypes.

2.3. Imaging and cerebrospinal fluid biomarkers in ADNI

To measure hippocampal and intracranial volumes from T1-weighted brain MRI scans, we used FreeSurfer version 5.1 (surfer.nmr.mgh.harvard.edu) (Jack et al., 2010). For assessment of cortical amyloid accumulation, we used preprocessed (coregistered, averaged, standardized image and voxel size, uniform resolution) [^{18}F] florbetapir PET scans (Jagust et al., 2015) and calculated mean standardized uptake values using a whole cerebellum reference region as previously described (Risacher et al., 2015). The concentration of CSF $A\beta_{42}$, p-tau, and t-tau was measured by the validated and highly automated Roche Elecsys electrochemiluminescence immunoassays (Roche Diagnostics, Mannheim, Germany) (Bittner et al., 2016).

2.4. Blood-based RNA expression microarray profiling

For the ADNI and AddNeuroMed samples, the PAXgene Blood RNA Kit (Qiagen Inc., Valencia, CA, USA) was used to purify total RNA from whole blood collected in a PAXgene Blood RNA Tube (Lunnon et al., 2012; Saykin et al., 2015). The Affymetrix Human Genome U219 Array (Affymetrix, Santa Clara, CA, USA) and the Illumina Human HT-12 v3 Expression BeadChips (Illumina Inc., San Diego, CA, USA) were used for expression profiling in ADNI and AddNeuroMed, respectively (Lunnon et al., 2012; Saykin et al., 2015). Raw expression values were preprocessed using the robust multichip average normalization method in ADNI (Choe et al., 2005) and the robust spline normalization method in AddNeuroMed (Du et al., 2008). We checked discrepancies between the reported sex and sex determined from sex-specific gene expression data including *XIST* and *USP9Y*. We also evaluated whether SNP genotypes were matched with genotypes predicted from gene expression data (Schadt et al., 2012). After QC, the RNA expression profiles contained 21,150 and 5141 probes, in ADNI and AddNeuroMed, respectively. The RNA expression profiles were pre-adjusted with RNA integrity number values and batch effects using linear regression.

2.5. Gene coexpression network analysis and identification of AD-related modules

We constructed clusters (modules) of highly coexpressed genes from RNA expression profiles of all participants (cognitively normal older adults (CN) and patients with MCI and AD) using the weighted correlation network analysis (WGCNA) software (Langfelder and Horvath, 2008), which calculates the network adjacency matrix based on coexpression similarity and identifies gene modules using unsupervised hierarchical clustering. Modules were represented by a weighted average expression profile, the module eigengene (ME), which is defined as the first principal component of the expression matrix in each module. We then performed a correlation analysis between ME and AD diagnosis (CN vs. AD) and presented this as a color-coded correlation map. We also performed a linear regression analysis with AD diagnosis, age and sex as independent variables and ME as an outcome to identify modules that were dysregulated in AD using R version 3.6.0 (www.R-project.org). Multiple testing correction was performed using the false discovery rate (FDR) with the Benjamini-Hochberg procedure (Benjamini and Hochberg, 1995).

2.6. Pathway-based enrichment analysis of AD-related modules

We performed enrichment analysis to identify the biological pathways of genes assigned to each of the AD-related modules. The DAVID bioinformatic resource was used to evaluate whether genes in a particular biological pathway were significantly more enriched in a given module than would be expected by random chance (FDR-corrected p-value < 0.05) (Huang et al., 2009). KEGG (Kyoto Encyclopedia of Genes and Genomes) pathways were used as a reference for functional annotation (Kanehisa et al., 2016). We then checked whether the biological pathways identified in ADNI were replicated in AddNeuroMed. We defined pathways as replicated only when the ME of the corresponding module in AddNeuroMed showed also a significant diagnosis group difference in the same direction (positively or negatively) as the ME of the matching ADNI module.

2.7. Module-based association analysis of modules with replicated biological pathways with AD biomarkers

We performed a linear regression analysis to evaluate whether the ME of AD-related modules that had the replicated biological pathways were also associated with the following AD biomarkers in all participants (CN, MCI, and AD) from the ADNI cohort (FDR-corrected p-value < 0.05): composite scores for memory and executive function (Crane et al.,; Gibbons et al.,), hippocampal volume on MRI, CSF $A\beta_{42}$, CSF p-tau, CSF t-tau, CSF p-tau/$A\beta_{42}$, CSF t-tau/$A\beta_{42}$, and averaged cortical uptake of [^{18}F] florbetapir PET. Covariates included age and sex. Intracranial volume and MRI field strength were also used as covariates for hippocampal volume.

2.8. Gene-based association analysis of target genes in replicated biological pathways

We selected common genes that belonged to each replicated biological pathway in both ADNI and AddNeuroMed. For each pathway, we identified genes that showed differential expression between AD and CN in ADNI and examined whether the findings were replicated in AddNeuroMed (FDR-corrected p-value < 0.05). For those differentially expressed genes, gene-based association analysis with AD biomarkers was performed using a set-based test in PLINK 1.9. SNPs in the coding region, 5′ untranslated region, 3′ untranslated region, regulatory region, and intronic region (±20 kb of upstream and downstream regions) with minor allele frequency greater than 0.05 were used for analysis. The same AD biomarkers in the module-based association analysis were used for this analysis as well. An empirical p-value (20,000 permutation) was calculated for each gene.

2.9. eQTL analysis of differentially expressed genes

We performed eQTL analysis on differentially expressed genes in each replicated biological pathway using PLINK 1.9 (FDR-corrected p-value < 0.05) (Rockman and Kruglyak, 2006). The GWAS and RNA expression data from all participants (CN, MCI, and AD) with the same set of SNPs for each gene in the gene-based association analysis were used for eQTL analysis. We then checked whether the significantly associated SNPs were replicated in AddNeuroMed. In addition, we performed a meta-analysis using METAL (Willer et al., 2010), which weighted the effect size estimates by their estimated standard errors. Results of the eQTL analysis were plotted using LocusZoom (Pruim et al., 2010).

2.10. Hub genes in AD-related modules with the replicated biological pathways

We identified hub genes (top 10% of genes with the highest intramodular connectivity) and the overlapping hub genes for the AD-related modules with replicated biological pathways in ADNI and AddNeuroMed using WGCNA.

3. Results

A total of 661 participants from ADNI and 674 participants from AddNeuroMed were included in the present study (Table 1). Gene coexpression network analysis using WGCNA yielded 17 and 13 modules of highly coexpressed genes in ADNI and AddNeuroMed, respectively (Fig. 1). Following a linear regression analysis, 4 modules (lightgreen, red, brown and darkturquoise) in ADNI and 5 modules (turquoise, yellow, black, tan and green) in AddNeuroMed were significantly dysregulated in AD compared with control samples (FDR-corrected p-value < 0.05) (Supplementary Table A1).

Pathway-based enrichment analysis of the 4 AD-related modules in ADNI identified a total of 10 enriched biological pathways (Table 2). Among them, 3 pathways linked to the brown module (containing 1580 genes) in ADNI were replicated in the yellow module (containing 466 genes) of AddNeuroMed (FDR-corrected p-value < 0.05): Fc gamma receptor (FcγR)-mediated phagocytosis, osteoclast differentiation, and tuberculosis. The ribosome pathway was also enriched in both the red module of ADNI and the turquoise module of AddNeuroMed. However, it was not considered to be replicated because the direction of the relationship between the ME and AD diagnosis was opposite in ADNI and AddNeuroMed. Therefore, only the brown module in ADNI and the yellow module in AddNeuroMed had the replicated biological pathways in the enrichment analysis. Module-based association analysis revealed that the brown module in ADNI was positively

Table 1
Demographics of study population

Cohort	Diagnosis	No. of participants	Female (%)	Age, mean (SD)	RIN, mean (SD)
ADNI (N = 661)	CN	213	107 (50%)	76.4 (6.4)	6.91 (0.51)
	MCI	345	144 (42%)	73.2 (7.9)	6.98 (0.55)
	AD	103	38 (37%)	77.6 (7.8)	6.98 (0.64)
AddNeuroMed (N = 674)	CN	243	147 (60%)	74.2 (6.6)	8.96 (0.73)
	MCI	208	120 (58%)	75.5 (6.5)	8.50 (0.59)
	AD	223	146 (65%)	76.8 (6.8)	8.43 (0.64)

Key: AD, Alzheimer's disease; CN, cognitively normal older adults; MCI, mild cognitive impairment; RIN, RNA integrity number; SD, standard deviation.

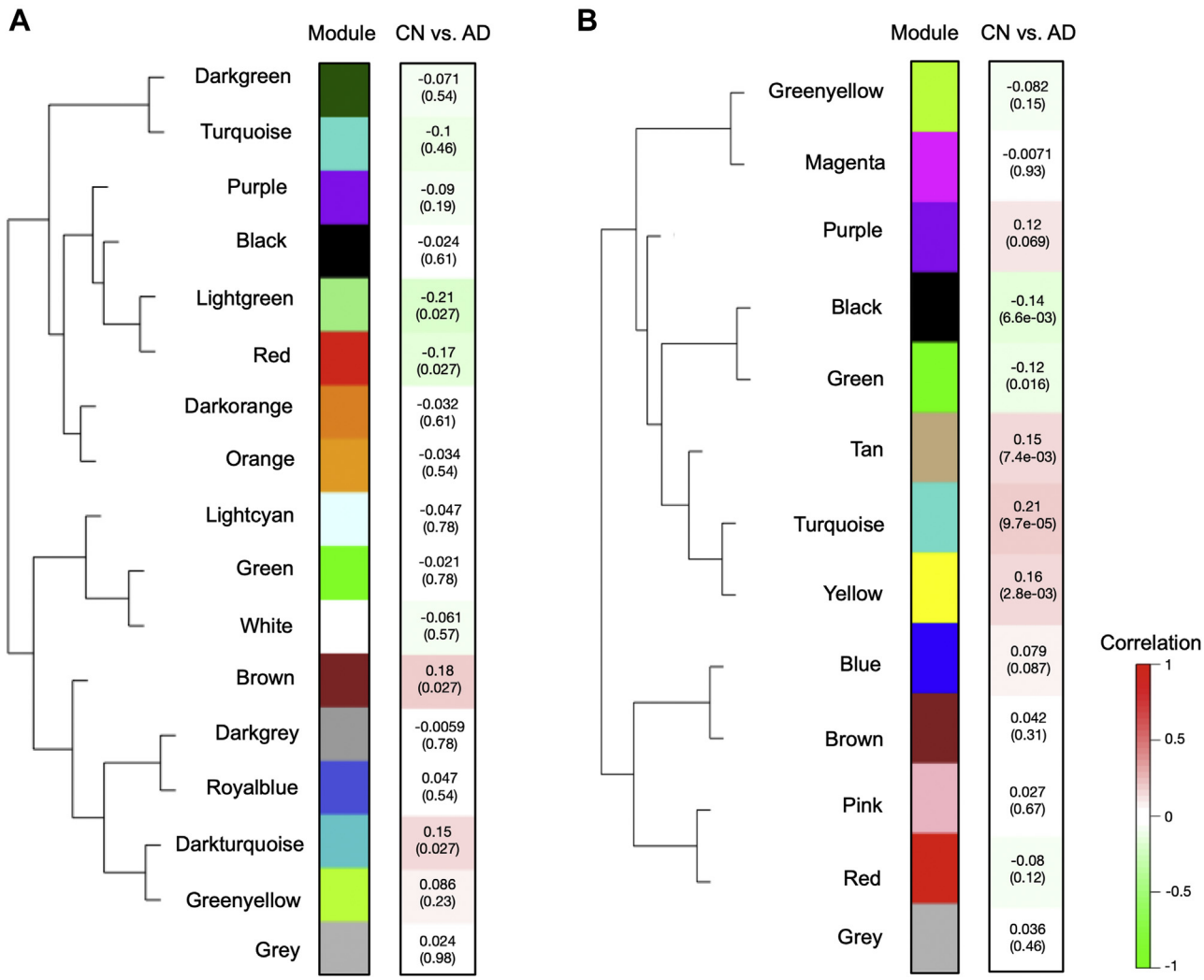

Fig. 1. Clustering dendrogram with correlation between modules and AD diagnosis (CN vs. AD). Weighted correlation network analysis constructed 17 and 13 modules in ADNI (A; discovery data) and AddNeuroMed (B; replication data) cohorts, respectively. The modules are represented in the rows with the clustering dendrogram. Colors were assigned to the modules arbitrarily according to their size by the WGCNA software. Each cell contains the correlation between the corresponding module and AD diagnosis (CN vs. AD) with its FDR-corrected *p*-value. It is color-coded by the correlation according to the color legend. The *p*-value was derived from a linear regression analysis with AD diagnosis, age, and sex as independent variables and module eigengene as an outcome. Abbreviations: AD, Alzheimer's disease; CN, cognitively normal older adults; FDR, false discovery rate; WGCNA, weighted correlation network analysis. (For interpretation of the references to color in this figure legend, the reader is referred to the Web version of this article.)

associated with mean cortical Aβ accumulation measured using [^{18}F] florbetapir PET scans and negatively associated with composite scores for memory and executive function as well as hippocampal volume (Table 3 and Fig. 2).

In the FcγR-mediated phagocytosis pathway, we identified 11 genes (*ASAP1, GAB2, LYN, MAPK1, MAPK3, MARCKS, PAK1, PLCG2, PRKCD, SYK,* and *VASP*) that were common in both the brown module of ADNI and the yellow module of AddNeuroMed. In ADNI, *ASAP1*, *PRKCD,* and *VASP* were significantly overexpressed in AD compared with CN. Among the 3 genes, *ASAP1* and *PRKCD* were replicated in AddNeuroMed. Gene-based association analysis of SNPs within *ASAP1* and *PRKCD* with AD biomarkers identified *PRKCD* as being significantly associated with cognitive functions and CSF p-tau/Aβ_{42} (Table 4). eQTL analysis identified several SNPs in *ASAP1* as being associated with expression levels of *ASAP1*, which were replicated in AddNeuroMed. rs11774659 had the lowest *p*-value of 4.81×10^{-9} in the meta-analysis. We plot each SNP in the region on the chromosome and indicate their association with *ASAP1* expression levels (Fig. 3). No SNPs were identified and replicated in *PRKCD*.

In the osteoclast differentiation pathway, we identified 15 genes (*GAB2, GRB2, IFNAR1, LILRA2, LILRB2, LILRB3, MAPK1, MAPK3, OSCAR, PLCG2, SIRPA, SPI1, SYK, TNFRSF1A,* and *TYROBP*) that were common in both the brown module of ADNI and the yellow module of AddNeuroMed. In ADNI, *LILRA2, LILRB3, SPI1,* and *TYROBP* were significantly overexpressed in AD compared with CN. Among them, 3 genes (*LILRA2, LILRB3,* and *TYROBP*) were replicated in AddNeuroMed. Gene-based association analysis of SNPs with AD biomarkers identified only *LILRB3* as being significantly associated with cognitive functions and CSF p-tau/Aβ_{42} (Table 4). eQTL analysis identified SNPs in *LILRA2* as significantly associated with expression levels of *LILRA2*, which was replicated in AddNeuroMed. rs28516458 had the smallest *p*-value of 5.42×10^{-18} in the meta-analysis (Fig. 3). No SNPs were identified and replicated in *LILRB3* and *TYROBP*.

In the tuberculosis pathway, we identified 14 common genes (*APAF1, ATP6V0B, ATP6V0D1, CAMK2G, CREBBP, CTSD, FADD, LSP1, MAPK1, MAPK3, RAB5C, RAB7A, SYK,* and *TNFRSF1A*) in both the brown module of ADNI and the yellow module of AddNeuroMed. *APAF1* were significantly overexpressed in AD compared with CN in ADNI, which was replicated in AddNeuroMed. Gene-based

Table 2
Biological pathways identified in enrichment analysis

Module (Direction of association between ME and diagnosis)	KEGG pathway	FDR-corrected *p*-value
ADNI		
Lightgreen (↓ME in AD)	B-cell receptor signaling	7.44×10^{-5}
Red (↓ME in AD)	Ribosome	3.35×10^{-21}
Brown (↑ME in AD)	Fc gamma receptor−mediated phagocytosis	8.49×10^{-4}
	Osteoclast differentiation	1.58×10^{-5}
	Tuberculosis	2.42×10^{-6}
	Endocytosis	2.51×10^{-2}
	B-cell receptor signaling	2.25×10^{-2}
	Hepatitis B	1.89×10^{-2}
	Lysosome	2.22×10^{-3}
	Estrogen signaling	1.98×10^{-2}
AddNeuroMed		
Yellow (↑ME in AD)	Fc gamma receptor−mediated phagocytosis	4.58×10^{-5}
	Osteoclast differentiation	2.31×10^{-7}
	Tuberculosis	4.26×10^{-5}
Turquoise (↑ME in AD)	Ribosome	3.25×10^{-17}

Values were derived from the DAVID bioinformatic resources (Huang et al., 2009).
No KEGG pathways were enriched at dark turquoise module in ADNI and black, green, and tan modules in AddNeuroMed (FDR-corrected p-value < 0.05).
In AddNeuroMed, we only demonstrated KEGG pathways which were identified in ADNI and were significantly enriched (FDR-corrected p-value < 0.05).
Key: AD, Alzheimer's disease; ME, module eigengene; ADNI, Alzheimer's Disease Neuroimaging Initiative; FDR, false discovery rate; KEGG, Kyoto Encyclopedia of Genes and Genomes.

association analysis of SNPs within *APAF1* did not identify any associations between SNPs and AD biomarkers. No SNPs in *APAF1* were identified and replicated in eQTL analysis.

In the intramodular connectivity analysis, we identified 160 and 58 hub genes from the brown module of ADNI and the yellow module of AddNeuroMed, respectively. A total of 30 genes, including *PRKCD* and *LILRB3*, overlapped between the 2 modules (Supplementary Table A2).

4. Discussion

In this study, we constructed modules from gene coexpression network analysis in peripheral blood and determined that 3 biological pathways (FcγR-mediated phagocytosis, osteoclast differentiation, and tuberculosis) were dysregulated in patients with AD. The brown module in ADNI in which these 3 pathways were found was associated with AD biomarkers including cognitive functions, hippocampal volume, and cortical Aβ accumulation. This is the first blood-based transcriptomic study in AD that used 2 independent cohorts (discovery and replication samples) to demonstrate consistent findings.

FcγRs, which are cellular receptors for IgG, play an important role in various types of immune responses. One function is to couple the specificity of the antibody response to innate effector pathways, such as phagocytosis, antibody-dependent cellular cytotoxicity, and the recruitment, and activation of inflammatory cells (Nimmerjahn and Ravetch, 2006). It is known that FcγRs are necessary for the intracerebral immune complex to induce inflammation in the brain (Teeling et al., 2012). The increased expression of FcγRs on microglia has been observed in both animal models and patients with AD (Fuller et al., 2014). Indeed, it is through this mechanism that antibodies against Aβ peptide may trigger microglia to clear Aβ plaques and thus cause the serious side effects called amyloid-related imaging abnormalities when using such immunotherapy strategies (Gu et al., 2016; Lai et al., 2017; Le Page et al., 2018). It is possible to prevent these outcomes by neutralizing the Fc arm of the antibody without loss of efficacy as Aβ plaques can be neutralized by Aβ antibodies without the action of Fc receptors (Das et al., 2003; Golde et al., 2009).

Interestingly, in vitro phagocytic activity by peripheral blood monocytes was significantly increased in participants with amyloid-positive PET scans compared with participants with amyloid-negative PET scans (Gu et al., 2016). Peripheral inflammatory markers were found to be elevated in patients with AD as well (Lai et al., 2017). Inflammation initiated in the brain may lead to the release of soluble inflammatory mediators that migrate to the periphery and activate peripheral immune cells (Le Page et al., 2018). On the other hand, these peripheral immune cells may also migrate to the brain and perpetuate brain inflammation through the disrupted blood-brain barrier in AD, sustaining a vicious cycle between the brain and periphery (Le Page et al., 2018; Sweeney et al., 2018).

We also found that *ASAP1* and *PRKCD* were significantly overexpressed in patients with AD compared to CN among genes in the FcγR-mediated phagocytosis pathway. In linkage analysis of autopsy-confirmed familial AD, it was reported that some SNPs near *ASAP1* were associated with AD (Sillén et al., 2011). In addition, *PRKCD* encodes protein kinase C-δ which is activated by Aβ and phosphorylates myristoylated alanine-rich C kinase substrate (Nakai et al., 2001). The phosphorylation of myristoylated alanine-rich C kinase substrate is known to induce neurite degeneration via instability of the actin network in human and mouse brains (Fujita et al., 2016).

Osteoclasts are bone-resorbing cells that regulate bone turnover (Cappariello et al., 2014). It was known that low bone mineral density was associated with the risk of AD (Tan et al., 2005). Previously, the association between AD and osteoporosis was thought to be related to reduced daily activities, low vitamin D, or low

Table 3
Association between the brown module of ADNI and various AD biomarkers

AD biomarker	*t*-value	FDR-corrected *p*-value
ADNI-EF[a]	−2.779	1.71×10^{-2}
ADNI-MEM	−2.677	1.71×10^{-2}
Hippocampal volume in MRI[b]	−3.148	1.55×10^{-2}
Averaged cortical uptake of [^{18}F] florbetapir PET[c]	2.684	1.71×10^{-2}

t-values and *p*-values were derived from a linear regression analysis between module eigengene of the brown module and AD biomarkers.
Key: AD, Alzheimer's disease; ADNI-EF, composite score of executive function in ADNI; ADNI-MEM, Composite score of memory in ADNI; FDR, false discovery rate.
[a] Data for 2 participants were unavailable.
[b] Data for 44 participants were unavailable.
[c] Data for 99 participants were unavailable.

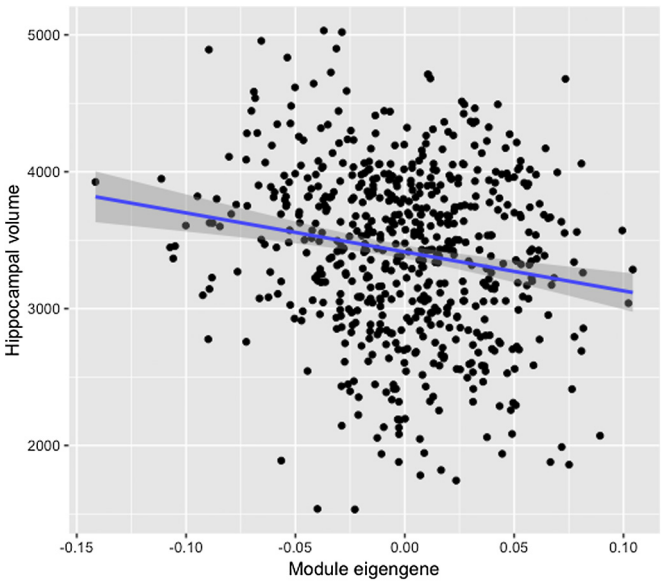

Fig. 2. Relationship between hippocampal volume and the brown module in ADNI. The relationship between hippocampal volume and module eigengene (ME) of the brown module in ADNI was represented in a scatter plot. The blue line was obtained from a linear regression analysis (FDR-corrected p-value = 1.55×10^{-2}), and the gray zone around the blue line indicates 95% confidence interval. Abbreviations: ADNI, Alzheimer's Disease Neuroimaging Initiative; FDR, false discovery rate. (For interpretation of the references to color in this figure legend, the reader is referred to the Web version of this article.)

estrogen exposure (Ensrud and Crandall, 2017; Mokry et al., 2016; Tan et al., 2005). However, it was also reported that differentiation of osteoclasts is increased in an AD mouse model, which favors loss of bone mineral (Cui et al., 2011). Furthermore, Aβ peptides were elevated in human osteoporotic bone tissues and enhanced osteoclast function (Li et al., 2014). The altered osteoclast differentiation pathway that we identified in peripheral blood of patients with AD might be associated with increased risk of osteoporosis in patients with AD.

Differentially expressed genes between AD and CN in the osteoclast differentiation pathway were related to the pathogenesis of patients with AD. TYRO protein tyrosine kinase-binding protein, encoded by *TYROBP*, is a signaling adaptor protein that plays important roles in signal transduction in microglia, osteoclasts, macrophages, and dendritic cells and enhances phagocytic activity of microglia (Ma et al., 2015). It was reported that *TYROBP* acted as a key regulator in an immune- and microglia-specific module that was constructed from the brain transcriptomic network of patients with AD (Zhang et al., 2013). Leukocyte Ig-like receptors are expressed on innate and adaptive immune cells and maintain immune homeostasis (Takeda and Nakamura, 2017). *LILRA2* was known to act as one of the hub genes in the Fc receptor system in the brain transcriptomic network of patients with AD (Zhang et al., 2013).

The tuberculosis pathway was also identified in the enrichment analysis. Some of the subpathways of the tuberculosis pathway, such as the toll-like receptor signaling pathway and the mitogen-activated protein kinase signaling pathway, are known to be associated with the pathogenesis of AD and may be of some influence (Huang et al., 2017; Kim and Choi, 2010).

For the past few decades, the amyloid cascade hypothesis has been accepted as the main pathophysiological mechanism of AD (Selkoe and Hardy, 2016). It states that the deposition of Aβ protein is the causative agent of Alzheimer's pathology and that the neurofibrillary tangles, cell loss, and cognitive decline follow as a direct result of this deposition (Hardy and Higgins, 1992). However, clinical trials that reduce brain amyloid in patients with AD have repeatedly failed, suggesting that another key mechanism, in addition to the Aβ deposition, is necessary to explain the occurrence and progression of AD (Mullane and Williams, 2018). Previously, neuroinflammation was considered to be merely a late-stage phenomenon in AD (Wyss-Coray, 2006); however, preclinical, genetic, and bioinformatic studies have shown that it actively contributes to AD pathogenesis and is now recognized as a core feature of AD (Heppner et al., 2015). Brain transcriptomic studies as well as several small blood transcriptomic studies have implicated the innate immune pathway in the pathogenesis of AD (International Genomics of Alzheimer's Disease Consortium, 2015; Zhang et al., 2013), which is summarized in a review article (Song et al., 2016).

This present study has some limitations. First, the regression coefficients observed in blood are relatively small in magnitude, compared with what is typically observed in postmortem brain studies. However, our findings were replicated in 2 independent data sets. Furthermore, while access to brain tissue from living patients is extremely limited, blood is easily accessible, noninvasive, and inexpensive and can be obtained longitudinally, providing a useful potential biomarker for AD. Second, blood-based transcriptomic profiles could be influenced by confounding factors such as medication and blood collection, processing, and storage procedures (Hampel et al., 2018; Mohr and Liew, 2007). However, we checked RNA quality using RNA integrity number values and also filtered out genes with low expression values. Importantly, we replicated our results using an independent data set. Third, transcriptome profiling was performed on different microarray platforms in ADNI and AddNeuroMed. Therefore, in this study, we did not perform a mega-analysis but constructed network-based modules in ADNI and AddNeuroMed separately. Although the present replicated results are robust, we may have not detected other potentially important peripheral transcriptomic changes because of methodological differences between cohorts. Fourth, we used expression profile technology. Newer RNA-sequencing methods in the future may better quantitate expression and clarify the role of other factors such as alternative splicing sites.

Table 4
Gene-based association analysis with AD biomarkers

AD biomarker	Gene set	No. of SNP	No. of significant SNP	Empirical p-value	Independent significant SNPs
ADNI-MEM	*PRKCD*	132	30	2.55×10^{-3}	rs6764111, rs11130350
ADNI-EF[a]	*PRKCD*	132	50	2.61×10^{-2}	rs6764111, rs62254274, rs3821689, rs2358617, rs12495976
CSF p-tau/$A\beta_{42}$[b]	*PRKCD*	132	43	4.18×10^{-2}	rs17052826, rs1872037, rs6778939, rs11130347, rs55685362
ADNI-MEM	*LILRB3*	216	9	6.25×10^{-3}	rs11878556, rs17841905, rs117107587
ADNI-EF[a]	*LILRB3*	216	22	1.50×10^{-2}	rs6509855, rs620207, rs11084325, rs4442928, rs16960152
CSF p-tau/$A\beta_{42}$[b]	*LILRB3*	216	10	3.88×10^{-2}	rs6509855, rs34810796, rs606851, rs202131060

Key: AD, Alzheimer's disease; $A\beta_{42}$, amyloid-β_{42}; ADNI-EF, composite score of executive function in ADNI; ADNI-MEM, composite score of memory in ADNI; p-tau, phosphorylated tau_{181p}.
[a] Data for 2 participants were unavailable.
[b] Data for 206 participants were unavailable.

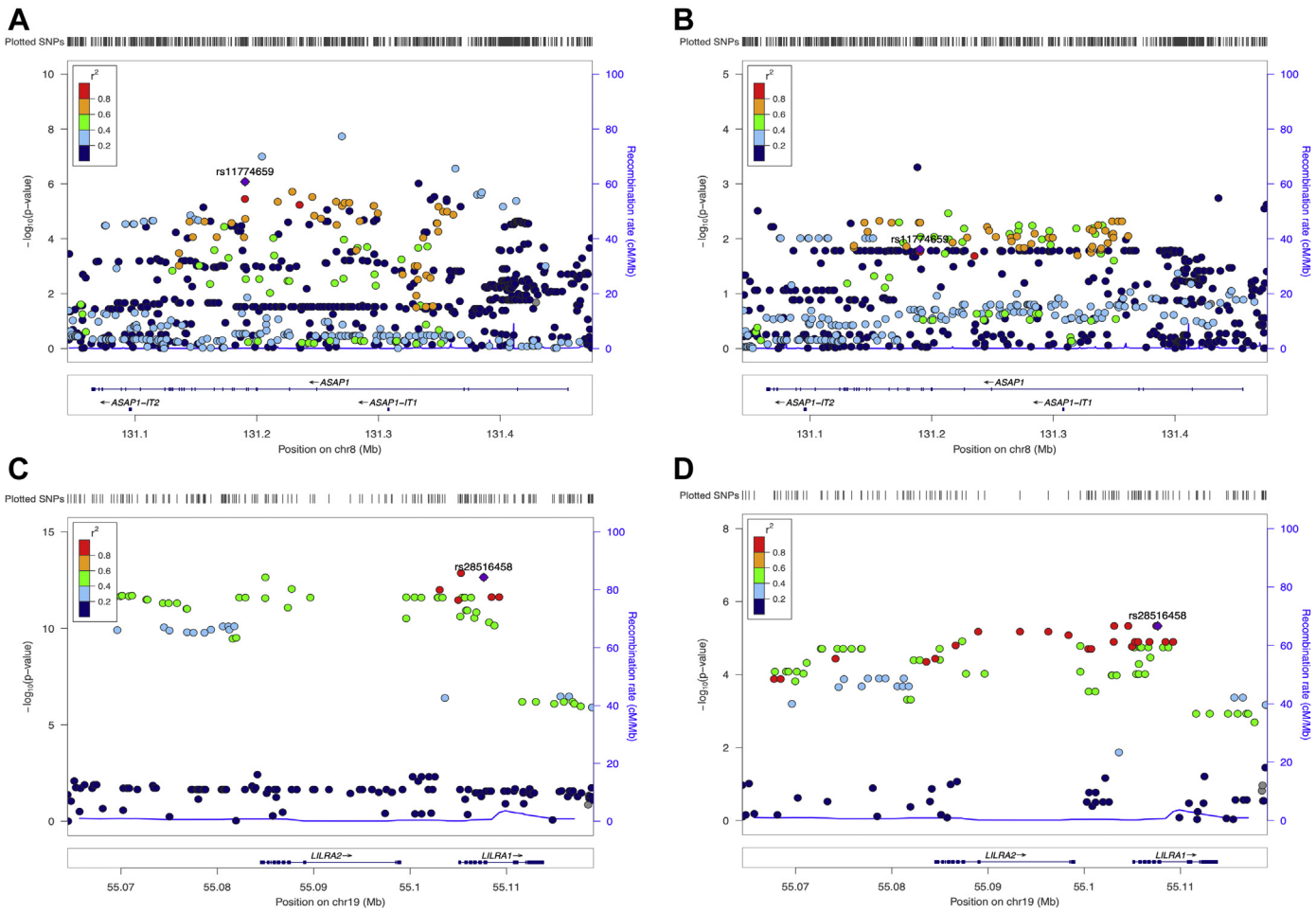

Fig. 3. LocusZoom plot for eQTL analysis of *ASAP1* and *LILRA2* SNPs' positions on chromosome and their color-coded association with expression levels of *ASAP1* are plotted in ADNI (A) and AddNeuroMed (B). The SNP with the lowest *p*-value in a meta-analysis (rs11774659) is indicated. The eQTL results of *LILRA2* are plotted for ADNI (C) and AddNeuroMed (D) with an indication of the SNP with the lowest *p*-value (rs28516458) in a meta-analysis. Abbreviations: eQTL, expression quantitative trait locus; SNP, single-nucleotide polymorphism. (For interpretation of the references to color in this figure legend, the reader is referred to the Web version of this article.)

Finally, we analyzed cross-sectionally collected gene expression data. Thus, our findings represent association not causality. Longitudinal studies are needed to understand the role of altered pathways in the onset of AD as well as cause and effect relationships.

In summary, network-based blood gene expression analysis showed that dysregulated pathways, including FcγR-mediated phagocytosis, were observed in patients with AD. Transcriptomics can provide a comprehensive understanding of biological processes and hold great promise for personalized and precision medicine (Li et al., 2016). With more sophisticated blood transcriptome profiling methods and integrative analysis approaches with validation using other multiomics data, blood-based transcriptomics profiles may become suitable for use in clinical practice for predicting, diagnosing, and personalizing treatment for AD.

Disclosure statement

The authors have no conflict of interest to report.

CRediT authorship contribution statement

Young Ho Park: Methodology, Software, Validation, Investigation, Writing - original draft, Writing - review & editing, Visualization. **Angela Hodges:** Validation, Resources, Data curation. **Shannon L. Risacher:** Resources, Data curation. **Kuang Lin:** Resources. **Jae-Won Jang:** Software. **Soyeon Ahn:** Software. **SangYun Kim:** Supervision. **Simon Lovestone:** Resources. **Andrew Simmons:** Resources. **Michael W. Weiner:** Resources. **Andrew J. Saykin:** Writing - original draft, Writing - review & editing, Supervision. **Kwangsik Nho:** Conceptualization, Methodology, Writing - original draft, Writing - review & editing, Supervision, Project administration.

Acknowledgements

Data collection and sharing for this project was funded by the Alzheimer's Disease Neuroimaging Initiative (National Institutes of Health Grant U01 AG024904) and DOD ADNI (Department of Defense award number W81XWH-12-2-0012). ADNI is funded by the National Institute on Aging, the National Institute of Biomedical Imaging and Bioengineering, and through generous contributions from the following: AbbVie, Alzheimer's Association; Alzheimer's Drug Discovery Foundation; Araclon Biotech; BioClinica, Inc.; Biogen; Bristol-Myers Squibb Company; CereSpir, Inc.; Cogstate; Eisai Inc.; Elan Pharmaceuticals, Inc.; Eli Lilly and Company; EuroImmun; F. Hoffmann-La Roche Ltd and its affiliated company Genentech, Inc.; Fujirebio; GE Healthcare; IXICO Ltd.; Janssen Alzheimer Immunotherapy Research & Development, LLC.; Johnson & Johnson

Pharmaceutical Research & Development LLC.; Lumosity; Lundbeck; Merck & Co., Inc.; Meso Scale Diagnostics, LLC.; NeuroRx Research; Neurotrack Technologies; Novartis Pharmaceuticals Corporation; Pfizer Inc.; Piramal Imaging; Servier; Takeda Pharmaceutical Company; and Transition Therapeutics. The Canadian Institutes of Health Research is providing funds to support ADNI clinical sites in Canada. Private sector contributions are facilitated by the Foundation for the National Institutes of Health (www.fnih.org). The grantee organization is the Northern California Institute for Research and Education, and the study is coordinated by the Alzheimer's Therapeutic Research Institute at the University of Southern California. ADNI data are disseminated by the Laboratory for Neuro Imaging at the University of Southern California. The collection and analysis of AddNeuroMed samples was supported by InnoMed (Innovative Medicines in Europe) an Integrated Project funded by the European Union of the Sixth Framework program priority FP6-2004-LIFESCIHEALTH-5, the Alzheimer's Research Trust, the John and Lucille van Geest Foundation and the NIHR Biomedical Research Centre for Mental Health at the South London and Maudsley NHS Foundation Trust and [Institute of Psychiatry] Kings College London.

Additional support for data analysis was provided by NLM R01 LM012535, NIA R03 AG054936, NIA R01 AG19771, NIA P30 AG10133, NLM R01 LM011360, DOD W81XWH-14-2-0151, NIGMS P50GM115318, NCATS UL1 TR001108, NIA K01 AG049050, the Alzheimer's Association, the Indiana Clinical and Translational Science Institute, and the IU Health-IU School of Medicine Strategic Neuroscience Research Initiative.

Appendix A. Supplementary data

Supplementary data to this article can be found online at https://doi.org/10.1016/j.neurobiolaging.2019.12.001.

References

Alzheimer's Association, 2018. Alzheimer's disease facts and figures. Alzheimers Dement. 14, 367–429.

Bai, Z., Stamova, B., Xu, H., Ander, B.P., Wang, J., Jickling, G.C., Zhan, X., Liu, D., Han, G., Jin, L.W., Decarli, C., Lei, H., Sharp, F.R., 2014. Distinctive RNA expression profiles in blood associated with Alzheimer disease after accounting for white matter hyperintensities. Alzheimer Dis. Assoc. Disord. 28, 226–233.

Benjamini, Y., Hochberg, Y., 1995. Controlling the false discovery rate: a practical and powerful approach to multiple testing. J. R. Statist. Soc. 57, 289–300.

Bittner, T., Zetterberg, H., Teunissen, C.E., Ostlund, R.E., Militello, M., Andreasson, U., Hubeek, I., Gibson, D., Chu, D.C., Eichenlaub, U., Heiss, P., Kobold, U., Leinenbach, A., Madin, K., Manuilova, E., Rabe, C., Blennow, K., 2016. Technical performance of a novel, fully automated electrochemiluminescence immunoassay for the quantitation of β-amyloid (1-42) in human cerebrospinal fluid. Alzheimers Dement. 12, 517–526.

Booij, B.B., Lindahl, T., Wetterberg, P., Skaane, N.V., Sæbø, S., Feten, G., Rye, P.D., Kristiansen, L.I., Hagen, N., Jensen, M., Bårdsen, K., Winblad, B., Sharma, P., Lönneborg, A., 2011. A gene expression pattern in blood for the early detection of Alzheimer's disease. J. Alzheimers Dis. 23, 109–119.

Cappariello, A., Maurizi, A., Veeriah, V., Teti, A., 2014. The great Beauty of the osteoclast. Arch. Biochem. Biophys. 558, 70–78.

Chen, K.D., Chang, P.T., Ping, Y.H., Lee, H.C., Yeh, C.W., Wang, P.N., 2011. Gene expression profiling of peripheral blood leukocytes identifies and validates ABCB1 as a novel biomarker for Alzheimer's disease. Neurobiol. Dis. 43, 698–705.

Choe, S.E., Boutros, M., Michelson, A.M., Church, G.M., Halfon, M.S., 2005. Preferred analysis methods for Affymetrix GeneChips revealed by a wholly defined control dataset. Gen. Biol. 6, R16.

Crane, P.K., Carle, A., Gibbons, L.E., Insel, P., Mackin, R.S., Gross, A., Jones, R.N., Mukherjee, S., Curtis, S.M., Harvey, D., Weiner, M., Mungas, D., Alzheimer's disease neuroimaging initiative, 2012. Development and assessment of a composite score for memory in the Alzheimer's disease neuroimaging initiative (ADNI). Brain Imaging Behav 6, 502–516.

Cui, S., Xiong, F., Hong, Y., Jung, J.U., Li, X.S., Liu, J.Z., Yan, R., Mei, L., Feng, X., Xiong, W.C., 2011. APPswe/Aβ regulation of osteoclast activation and RAGE expression in an age-dependent manner. J. Bone Miner Res. 26, 1084–1098.

Das, P., Howard, V., Loosbrock, N., Dickson, D., Murphy, M.P., Golde, T.E., 2003. Amyloid-beta immunization effectively reduces amyloid deposition in FcR gamma(-/-) knock-out mice. J. Neurosci. 23, 8532–8538.

Dragomir, A., Vrahatis, A., Bezerianos, A., 2019. A network-based Perspective in Alzheimer's disease: current state and an integrative Framework. IEEE J. Biomed. Health Inform. 13, 14–25.

Du, P., Kibbe, W.A., Lin, S.M., 2008. Lumi: a pipeline for processing Illumina microarray. Bioinformatics 24, 1547–1548.

Eisen, M.B., Spellman, P.T., Brown, P.O., Botstein, D., 1998. Cluster analysis and display of genome-wide expression patterns. Proc. Natl. Acad. Sci. U. S. A. 95, 14863–14868.

Ensrud, K.E., Crandall, C.J., 2017. Osteoporos. Ann. Intern. Med. 167, ITC17–ITC32.

Fehlbaum-Beurdeley, P., Sol, O., Désiré, L., Touchon, J., Dantoine, T., Vercelletto, M., Gabelle, A., Jarrige, A.C., Haddad, R., Lemarié, J.C., Zhou, W., Hampel, H., Einstein, R., Vellas, B., EHTAD/002 Study Group, 2012. Validation of AclarusDx™, a blood-based transcriptomic signature for the diagnosis of Alzheimer's disease. J. Alzheimers Dis. 32, 169–181.

Fujita, K., Motoki, K., Tagawa, K., Chen, X., Hama, H., Nakajima, K., Homma, H., Tamura, T., Watanabe, H., Katsuno, M., Matsumi, C., Kajikawa, M., Saito, T., Saido, T., Sobue, G., Miyawaki, A., Okazawa, H., 2016. HMGB1, a pathogenic molecule that induces neurite degeneration via TLR4-MARCKS, is a potential therapeutic target for Alzheimer's disease. Sci. Rep. 6, 31895.

Fuller, J.P., Stavenhagen, J.B., Teeling, J.L., 2014. New roles for Fc receptors in neurodegeneration-the impact on Immunotherapy for Alzheimer's Disease. Front. Neurosci. 8, 235.

Furney, S.J., Simmons, A., Breen, G., Pedroso, I., Lunnon, K., Proitsi, P., Hodges, A., Powell, J., Wahlund, L.O., Kloszewska, I., Mecocci, P., Soininen, H., Tsolaki, M., Vellas, B., Spenger, C., Lathrop, M., Shen, L., Kim, S., Saykin, A.J., Weiner, M.W., Lovestone, S., 2011. Genome-wide association with MRI atrophy measures as a quantitative trait locus for Alzheimer's disease. Mol. Psychiatry 16, 1130–1138.

Gibbons, L.E., Carle, A.C., Mackin, R.S., Harvey, D., Mukherjee, S., Insel, P., Curtis, S.M., Mungas, D., Crane, P.K., Alzheimer's Disease Neuroimaging Initiative, 2012. A composite score for executive functioning, validated in Alzheimer's Disease Neuroimaging Initiative (ADNI) participants with baseline mild cognitive impairment. Brain Imaging Behav. 6, 517–527.

Gladkevich, A., Kauffman, H.F., Korf, J., 2004. Lymphocytes as a neural probe: potential for studying psychiatric disorders. Prog. Neuropsychopharmacol. Biol. Psychiatry 28, 559–576.

Golde, T.E., Das, P., Levites, Y., 2009. Quantitative and mechanistic studies of Abeta immunotherapy. CNS Neurol. Disord. Drug Targets 8, 31–49.

Gu, B.J., Huang, X., Ou, A., Rembach, A., Fowler, C., Avula, P.K., Horton, A., Doecke, J.D., Villemagne, V.L., Macaulay, S.L., Maruff, P., Fletcher, E.L., Guymer, R., Wiley, J.S., Masters, C.L., 2016. Innate phagocytosis by peripheral blood monocytes is altered in Alzheimer's disease. Acta Neuropathol. 132, 377–389.

Hampel, H., O'Bryant, S.E., Molinuevo, J.L., Zetterberg, H., Masters, C.L., Lista, S., Kiddle, S.J., Batrla, R., Blennow, K., 2018. Blood-based biomarkers for Alzheimer disease: mapping the road to the clinic. Nat. Rev. Neurol. 14, 639–652.

Han, G., Wang, J., Zeng, F., Feng, X., Yu, J., Cao, H.Y., Yi, X., Zhou, H., Jin, L.W., Duan, Y., Wang, Y.J., Lei, H., 2013. Characteristic transformation of blood transcriptome in Alzheimer's disease. J. Alzheimers Dis. 35, 373–386.

Hardy, J.A., Higgins, G.A., 1992. Alzheimers disease: the amyloid cascade hypothesis. Science 256, 184–185.

Heppner, F.L., Ransohoff, R.M., Becher, B., 2015. Immune attack: the role of inflammation in Alzheimer disease. Nat. Rev. Neurosci. 16, 358–372.

Huang, D.W., Sherman, B.T., Lempicki, R.A., 2009. Systematic and integrative analysis of large gene lists using DAVID bioinformatics resources. Nat. Protoc. 4, 44–57.

Huang, N.Q., Jin, H., Zhou, S.Y., Shi, J.S., Jin, F., 2017. TLR4 is a link between diabetes and Alzheimer's disease. Behav. Brain Res. 316, 234–244.

International Genomics of Alzheimer's Disease Consortium, 2015. Convergent genetic and expression data implicate immunity in Alzheimer's disease. Alzheimers Dement. 11, 658–671.

Jack, C.R., Bernstein, M.A., Borowski, B.J., Gunter, J.L., Fox, N.C., Thompson, P.M., Schuff, N., Krueger, G., Killiany, R.J., DeCarli, C.S., Dale, A.M., Carmichael, O.W., Tosun, D., Weiner, M.W., Alzheimer's Disease Neuroimaging Initiative, 2010. Update on the magnetic resonance imaging core of the Alzheimer's disease neuroimaging initiative. Alzheimers Dement. 6, 212–220.

Jagust, W.J., Landau, S.M., Koeppe, R.A., Reiman, E.M., Chen, K., Mathis, C.A., Price, J.C., Foster, N.L., Wang, A.Y., 2015. The Alzheimer's disease neuroimaging initiative 2 PET core: 2015. Alzheimers Dement. 11, 757–771.

Kanehisa, M., Sato, Y., Kawashima, M., Furumichi, M., Tanabe, M., 2016. KEGG as a reference resource for gene and protein annotation. Nucleic Acids Res. 44, D457–D462.

Kálmán, J., Kitajka, K., Pákáski, M., Zvara, A., Juhász, A., Vincze, G., Janka, Z., Puskás, L.G., 2005. Gene expression profile analysis of lymphocytes from Alzheimer's patients. Psychiatr. Genet. 15, 1–6.

Kang, J.H., Korecka, M., Figurski, M.J., Toledo, J.B., Blennow, K., Zetterberg, H., Waligorska, T., Brylska, M., Fields, L., Shah, N., Soares, H., Dean, R.A., Vanderstichele, H., Petersen, R.C., Aisen, P.S., Saykin, A.J., Weiner, M.W., Trojanowski, J.Q., Shaw, L.M., 2015. The Alzheimer's disease neuroimaging initiative 2 biomarker core: a review of progress and plans. Alzheimers Dement. 11, 772–791.

Kim, E.K., Choi, E.J., 2010. Pathological roles of MAPK signaling pathways in human diseases. Biochim. Biophys. Acta 1802, 396–405.

Lai, K.S.P., Liu, C.S., Rau, A., Lanctôt, K.L., Köhler, C.A., Pakosh, M., Carvalho, A.F., Herrmann, N., 2017. Peripheral inflammatory markers in Alzheimer's disease: a systematic review and meta-analysis of 175 studies. J. Neurol. Neurosurg. Psychiatry 88, 876–882.

Langfelder, P., Horvath, S., 2008. WGCNA: an R package for weighted correlation network analysis. BMC Bioinformatics 9, 559.
Le Page, A., Dupuis, G., Frost, E.H., Larbi, A., Pawelec, G., Witkowski, J.M., Fulop, T., 2018. Role of the peripheral innate immune system in the development of Alzheimer's disease. Exp. Gerontol. 107, 59–66.
Lee, Y., Han, S., Kim, D., Kim, D., Horgousluoglu, E., Risacher, S.L., Saykin, A.J., Nho, K., 2018. Genetic variation affecting exon skipping contributes to brain structural atrophy in Alzheimer's disease. AMIA Jt. Summits Transl Sci. Proc. 2017, 124–131.
Li, S., Liu, B., Zhang, L., Rong, L., 2014. Amyloid beta peptide is elevated in osteoporotic bone tissues and enhances osteoclast function. Bone 61, 164–175.
Li, S., Todor, A., Luo, R., 2016. Blood transcriptomics and metabolomics for personalized medicine. Comput. Struct. Biotechnol. J. 14, 1–7.
Li, Y., Willer, C.J., Ding, J., Scheet, P., Abecasis, G.R., 2010. MaCH: using sequence and genotype data to estimate haplotypes and unobserved genotypes. Genet. Epidemiol. 34, 816–834.
Lovestone, S., Francis, P., Kloszewska, I., Mecocci, P., Simmons, A., Soininen, H., Spenger, C., Tsolaki, M., Vellas, B., Wahlund, L.O., Ward, M., 2009. AddNeuroMed–the European collaboration for the discovery of novel biomarkers for Alzheimer's disease. Ann. N. Y. Acad. Sci. 1180, 36–46.
Lunnon, K., Ibrahim, Z., Proitsi, P., Lourdusamy, A., Newhouse, S., Sattlecker, M., Furney, S., Saleem, M., Soininen, H., Kłoszewska, I., Mecocci, P., Tsolaki, M., Vellas, B., Coppola, G., Geschwind, D., Simmons, A., Lovestone, S., Dobson, R., Hodges, A., 2012. Mitochondrial dysfunction and immune activation are detectable in early Alzheimer's disease blood. J. Alzheimers Dis. 30, 685–710.
Lunnon, K., Sattlecker, M., Furney, S.J., Coppola, G., Simmons, A., Proitsi, P., Lupton, M.K., Lourdusamy, A., Johnston, C., Soininen, H., Kłoszewska, I., Mecocci, P., Tsolaki, M., Vellas, B., Geschwind, D., Lovestone, S., Dobson, R., Hodges, A., 2013. A blood gene expression marker of early Alzheimer's disease. J. Alzheimers Dis. 33, 737–753.
Ma, J., Jiang, T., Tan, L., Yu, J.T., 2015. TYROBP in Alzheimer's disease. Mol. Neurobiol. 51, 820–826.
Maes, O.C., Xu, S., Yu, B., Chertkow, H.M., Wang, E., Schipper, H.M., 2007. Transcriptional profiling of Alzheimer blood mononuclear cells by microarray. Neurobiol. Aging 28, 1795–1809.
McCarthy, S., Das, S., Kretzschmar, W., Delaneau, O., Wood, A.R., Teumer, A., Kang, H.M., Fuchsberger, C., Danecek, P., Sharp, K., Luo, Y., Sidore, C., Kwong, A., Timpson, N., Koskinen, S., Vrieze, S., Scott, L.J., Zhang, H., Mahajan, A., Veldink, J., Peters, U., Pato, C., van Duijn, C.M., Gillies, C.E., Gandin, I., Mezzavilla, M., Gilly, A., Cocca, M., Traglia, M., Angius, A., Barrett, J.C., Boomsma, D., Branham, K., Breen, G., Brummett, C.M., Busonero, F., Campbell, H., Chan, A., Chen, S., Chew, E., Collins, F.S., Corbin, L.J., Smith, G.D., Dedoussis, G., Dorr, M., Farmaki, A.-E., Ferrucci, L., Forer, L., Fraser, R.M., Gabriel, S., Levy, S., Groop, L., Harrison, T., Hattersley, A., Holmen, O.L., Hveem, K., Kretzler, M., Lee, J.C., McGue, M., Meitinger, T., Melzer, D., Min, J.L., Mohlke, K.L., Vincent, J.B., Nauck, M., Nickerson, D., Palotie, A., Pato, M., Pirastu, N., McInnis, M., Richards, J.B., Sala, C., Salomaa, V., Schlessinger, D., Schoenherr, S., Slagboom, P.E., Small, K., Spector, T., Stambolian, D., Tuke, M., Tuomilehto, J., van den Berg, L.H., Van Rheenen, W., Volker, U., Wijmenga, C., Toniolo, D., Zeggini, E., Gasparini, P., Sampson, M.G., Wilson, J.F., Frayling, T., de Bakker, P.I.W., Swertz, M.A., McCarroll, S., Kooperberg, C., Dekker, A., Altshuler, D., Willer, C., Iacono, W., Ripatti, S., Soranzo, N., Walter, K., Swaroop, A., Cucca, F., Anderson, C.A., Myers, R.M., Boehnke, M., McCarthy, M.I., Durbin, R., Haplotype Reference Consortium, 2016. A reference panel of 64,976 haplotypes for genotype imputation. Nat. Genet. 48, 1279–1283.
McKhann, G., Drachman, D., Folstein, M., Katzman, R., Price, D., Stadlan, E.M., 1984. Clinical diagnosis of Alzheimer's disease: report of the NINCDS-ADRDA work group under the auspices of Department of Health and human Services Task force on Alzheimer's disease. Neurology 34, 939–944.
Mohr, S., Liew, C.C., 2007. The peripheral-blood transcriptome: new insights into disease and risk assessment. Trends Mol. Med. 13, 422–432.
Mokry, L.E., Ross, S., Morris, J.A., Manousaki, D., Forgetta, V., Richards, J.B., 2016. Genetically decreased vitamin D and risk of Alzheimer disease. Neurology 87, 2567–2574.
Morris, J.K., Honea, R.A., Vidoni, E.D., Swerdlow, R.H., Burns, J.M., 2014. Is Alzheimer's disease a systemic disease? Biochim. Biophys. Acta 1842, 1340–1349.
Mullane, K., Williams, M., 2018. Alzheimer's disease (AD) therapeutics - 1: Repeated clinical failures continue to question the amyloid hypothesis of AD and the current understanding of AD causality. Biochem. Pharmacol. 158, 359–375.
Nakai, M., Tanimukai, S., Yagi, K., Saito, N., Taniguchi, T., Terashima, A., Kawamata, T., Yamamoto, H., Fukunaga, K., Miyamoto, E., Tanaka, C., 2001. Amyloid beta protein activates PKC-delta and induces translocation of myristoylated alanine-rich C kinase substrate (MARCKS) in microglia. Neurochem. Int. 38, 593–600.
Naughton, B.J., Duncan, F.J., Murrey, D.A., Meadows, A.S., Newsom, D.E., Stoicea, N., White, P., Scharre, D.W., Mccarty, D.M., Fu, H., 2015. Blood genome-wide transcriptional profiles reflect broad molecular impairments and strong blood-brain links in Alzheimer's disease. J. Alzheimers Dis. 43, 93–108.
Nimmerjahn, F., Ravetch, J.V., 2006. Fcgamma receptors: old friends and new family members. Immunity 24, 19–28.
Potkin, S.G., Guffanti, G., Lakatos, A., Turner, J.A., Kruggel, F., Fallon, J.H., Saykin, A.J., Orro, A., Lupoli, S., Salvi, E., Weiner, M., Macciardi, F., 2009. Hippocampal atrophy as a quantitative trait in a genome-wide association study identifying novel Susceptibility genes for Alzheimer's disease. PLoS One 4, e6501.
Price, A.L., Patterson, N.J., Plenge, R.M., Weinblatt, M.E., Shadick, N.A., Reich, D., 2006. Principal components analysis corrects for stratification in genome-wide association studies. Nat. Genet. 38, 904–909.
Pruim, R.J., Welch, R.P., Sanna, S., Teslovich, T.M., Chines, P.S., Gliedt, T.P., Boehnke, M., Abecasis, G.R., Willer, C.J., 2010. LocusZoom: regional visualization of genome-wide association scan results. Bioinformatics 26, 2336–2337.
Purcell, S., Neale, B., Todd-Brown, K., Thomas, L., Ferreira, M.A.R., Bender, D., Maller, J., Sklar, P., de Bakker, P.I.W., Daly, M.J., Sham, P.C., 2007. PLINK: a tool set for whole-genome association and population-based linkage analyses. Am. J. Hum. Genet. 81, 559–575.
Ramanan, V.K., Risacher, S.L., Nho, K., Kim, S., Swaminathan, S., Shen, L., Foroud, T.M., Hakonarson, H., Huentelman, M.J., Aisen, P.S., Petersen, R.C., Green, R.C., Jack, C.R., Koeppe, R.A., Jagust, W.J., Weiner, M.W., Saykin, A.J., 2014. *APOE* and *BCHE* as modulators of cerebral amyloid deposition: a florbetapir PET genome-wide association study. Mol. Psychiatry 19, 351–357.
Risacher, S.L., Kim, S., Nho, K., Foroud, T., Shen, L., Petersen, R.C., Jack, C.R., Beckett, L.A., Aisen, P.S., Koeppe, R.A., Jagust, W.J., Shaw, L.M., Trojanowski, J.Q., Weiner, M.W., Saykin, A.J., Alzheimer's Disease Neuroimaging Initiative (ADNI), 2015. APOE effect on Alzheimer's disease biomarkers in older adults with significant memory concern. Alzheimers Dement. 11, 1417–1429.
Rockman, M.V., Kruglyak, L., 2006. Genetics of global gene expression. Nat. Rev. Genet. 7, 862–872.
Roed, L., Grave, G., Lindahl, T., Rian, E., Horndalsveen, P.O., Lannfelt, L., Nilsson, C., Swenson, F., Lönneborg, A., Sharma, P., Sjögren, M., 2013. Prediction of mild cognitive impairment that evolves into Alzheimer's disease dementia within two years using a gene expression signature in blood: a pilot study. J. Alzheimers Dis. 35, 611–621.
Rye, P.D., Booij, B.B., Grave, G., Lindahl, T., Kristiansen, L., Andersen, H.M., Horndalsveen, P.O., Nygaard, H.A., Naik, M., Hoprekstad, D., Wetterberg, P., Nilsson, C., Aarsland, D., Sharma, P., Lönneborg, A., 2011. A novel blood test for the early detection of Alzheimer's disease. J. Alzheimers Dis. 23, 121–129.
Saykin, A.J., Shen, L., Yao, X., Kim, S., Nho, K., Risacher, S.L., Ramanan, V.K., Foroud, T.M., Faber, K.M., Sarwar, N., Munsie, L.M., Hu, X., Soares, H.D., Potkin, S.G., Thompson, P.M., Kauwe, J.S.K., Kaddurah-Daouk, R., Green, R.C., Toga, A.W., Weiner, M.W., 2015. Genetic studies of quantitative MCI and AD phenotypes in ADNI: progress, opportunities, and plans. Alzheimers Dement. 11, 792–814.
Schadt, E.E., Woo, S., Hao, K., 2012. Bayesian method to predict individual SNP genotypes from gene expression data. Nat. Genet. 44, 603–608.
Selkoe, D.J., Hardy, J., 2016. The amyloid hypothesis of Alzheimer's disease at 25 years. EMBO Mol. Med. 8, 595–608.
Sillén, A., Brohede, J., Forsell, C., Lilius, L., Andrade, J., Odeberg, J., Kimura, T., Winblad, B., Graff, C., 2011. Linkage analysis of autopsy-confirmed familial Alzheimer disease supports an Alzheimer disease locus in 8q24. Dement. Geriatr. Cogn. Disord. 31, 109–118.
Song, F., Qian, Y., Peng, X., Han, G., Wang, J., Bai, Z., Crack, P.J., Lei, H., 2016. Perturbation of the transcriptome: implications of the innate immune system in Alzheimer's disease. Curr. Opin. Pharmacol. 26, 47–53.
Sweeney, M.D., Sagare, A.P., Zlokovic, B.V., 2018. Blood-brain barrier breakdown in Alzheimer disease and other neurodegenerative disorders. Nat. Rev. Neruol 14, 133–150.
Takeda, K., Nakamura, A., 2017. Regulation of immune and neural function via leukocyte Ig-like receptors. J. Biochem. 162, 73–80.
Tan, Z.S., Seshadri, S., Beiser, A., Zhang, Y., Felson, D., Hannan, M.T., Au, R., Wolf, P.A., Kiel, D.P., 2005. Bone mineral density and the risk of Alzheimer disease. Arch. Neurol. 62, 107–111.
Teeling, J.L., Carare, R.O., Glennie, M.J., Perry, V.H., 2012. Intracerebral immune complex formation induces inflammation in the brain that depends on Fc receptor interaction. Acta Neuropathol. 124, 479–490.
Thorisson, G.A., Smith, A.V., Krishnan, L., Stein, L.D., 2005. The International HapMap project Web site. Genome Res. 15, 1592–1593.
Tylee, D.S., Kawaguchi, D.M., Glatt, S.J., 2013. On the outside, looking in: a review and evaluation of the comparability of blood and brain "-omes". Am. J. Med. Genet. B Neuropsychiatr. Genet. 162B, 595–603.
Vidoni, E.D., Townley, R.A., Honea, R.A., Burns, J.M., 2011. Alzheimer disease biomarkers are associated with body mass index. Neurology 77, 1913–1920.
Willer, C.J., Li, Y., Abecasis, G.R., 2010. METAL: fast and efficient meta-analysis of genomewide association scans. Bioinformatics 26, 2190–2191.
Wyss-Coray, T., 2006. Inflammation in Alzheimer disease: driving force, bystander or beneficial response? Nat. Med. 12, 1005–1015.
Zhang, B., Gaiteri, C., Bodea, L.G., Wang, Z., McElwee, J., Podtelezhnikov, A.A., Zhang, C., Xie, T., Tran, L., Dobrin, R., Fluder, E., Clurman, B., Melquist, S., Narayanan, M., Suver, C., Shah, H., Mahajan, M., Gillis, T., Mysore, J., MacDonald, M.E., Lamb, J.R., Bennett, D.A., Molony, C., Stone, D.J., Gudnason, V., Myers, A.J., Schadt, E.E., Neumann, H., Zhu, J., Emilsson, V., 2013. Integrated systems approach identifies genetic nodes and networks in late-onset Alzheimer's disease. Cell 153, 707–720.